

ICANS XIV
14th Meeting of the International Collaboration on
Advanced Neutron Sources
June 14-19, 1998
Starved Rock Lodge, Utica, IL

**THERMAL NEUTRON SCATTERING KERNELS
FOR MODERATOR MATERIALS:
COMPARISON OF NJOY RESULTS FROM
A SYNTHETIC MODEL AND ITS STANDARD LIBRARY**

M.M. Scaffoni², V.H. Gillette¹, M.E. Pepe² and J.R. Granada^{1*}

Comisión Nacional de Energía Atómica
¹Centro Atómico Bariloche and Instituto Balseiro
²Centro Atómico Constituyentes
ARGENTINA

ABSTRACT

The Synthetic Scattering Function (SSF) allows a simple description of the incoherent interaction of slow neutrons with hydrogenous materials. The main advantages of this model reside in the analytical expressions that it produces for double-differential cross sections, energy-transfer kernels, and total cross sections, which in turn permit the fast evaluation of neutron scattering and transport properties.

We have included the SSF routines into the NJOY code, in such a way that the cross sections can be generated with the same format either from its standard library or from our synthetic model.

In this work we briefly discuss the basic features of the SSF, some details of its implementation into NJOY, and a few examples of results obtained using those two options.

* Also at CONICET, Argentina.

1. INTRODUCTION

The scattering function $S(\mathbf{Q}, \omega)$ is the central quantity to describe the interaction of thermal neutrons with condensed matter, as it contains all the dynamical and structural information about a scattering system [1]. First-principles theories were developed in the past to evaluate the scattering function, most of them based on the essentially exact Zemach-Glauber formalism [2], but the resulting expressions are usually not quite amenable for calculation.

In practice, and as far as neutron moderators are concerned, the compromise solution adopted in standard Nuclear Data Libraries involves the inclusion of scattering laws for a few common moderators at some selected temperatures, and data for any different material or physical condition must be 'constructed' from pieces of information actually corresponding to those few cases found in the existing files.

Those aspects were part of the main motivations for the development of a 'Synthetic Scattering Function' $T(\mathbf{Q}, \omega, E_0)$ [3], which incorporates the main dynamical characteristics of the molecular unit, still retaining a high degree of simplicity in its formulation. The characteristic features of the synthetic model have been recently reviewed [4], and we will just briefly discuss here some of its basic hypotheses and approximations.

2. THE MODEL

The synthetic scattering function has been developed to the extent of producing analytic forms for a variety of magnitudes [3,5], and their accuracy have been verified in a number of cases [6].

The incoherent double-differential scattering cross section of a molecular unit is written, in terms of the synthetic model, as [3]

$$\frac{\partial^2 \sigma}{\partial \Omega \partial E} = \sum_i^N n_i \frac{\sigma_b^i}{4\pi} T^i(\bar{\mathbf{Q}}, \omega, E_0) , \quad (1)$$

where N is the number of dynamically nonequivalent atomic species, and n_i represents the number of atoms of each equivalent atomic species with a bound scattering cross section σ_b . Finally, $T(\bar{\mathbf{Q}}, \omega, E_0)$ stands for the basic expression of the Synthetic Scattering Function (SSF):

$$T(\bar{\mathbf{Q}}, \omega, E_0) = \frac{k}{k_0} \left[S_{0, \tau_0, \Gamma}(\bar{\mathbf{Q}}, \omega) - \sum_{\lambda, \pm}^m C_{\lambda, \pm} \frac{\partial}{\partial \Gamma} S_{\mu_0, \tau_0, \Gamma}(\bar{\mathbf{Q}}_{\lambda, \pm}, \omega_{\lambda, \pm}) \right] , \quad (2)$$

where k_0 and k denote the modulus of incident and scattered neutron wave vectors, respectively, $\bar{\mathbf{Q}} = \bar{\mathbf{k}}_0 - \bar{\mathbf{k}}$ and $\hbar \omega = E_0 - E$ are the momentum and energy exchanged in the collision process. $S_{\mu_0, \tau_0, \Gamma}(\bar{\mathbf{Q}}, \omega)$ is the scattering law for the neutron interaction with a quasi-rigid molecule, and the second term on the right-hand side of Eq.(2) is a corrective one which accounts for processes where the neutron exchanges energy with the m internal modes of the atomic species, by creating or annihilating one phonon. The summation over inelastic processes is performed under the assumption that the internal modes are represented by Einstein oscillators, each with eigenfrequency ω_λ , and effective mass M_λ .

The quantities μ_0 , τ_0 and Γ represent the effective mass, temperature and vibrational factor, respectively, that the scattering nucleus would present in the interaction, and they depend explicitly on the incident neutron energy E_0 . In this manner, a kind of envelope represents the combined effect of the quantum excitations of the system's internal modes. Under those conditions, $S_{\mu_0, \tau_0, \Gamma}(\vec{Q}, \omega)$ may be written as

$$S_{\mu_0, \tau_0, \Gamma}(\vec{Q}, \omega) = \left[\frac{\mu_0}{2\pi \hbar^2 Q^2 k_B \tau_0} \right]^{0.5} \exp \left[- \left(\hbar\omega - \frac{\hbar^2 Q^2}{2\mu_0} \right)^2 \left(\frac{\mu_0}{2\hbar^2 Q^2 k_B \tau_0} \right) - \Gamma \frac{\hbar^2 Q^2}{2} \right] \quad (3)$$

The reduced number of input parameters required for the SSF and the analytic character of the derived expressions, make this formalism a powerful and practical tool for describing the slow neutron - molecule interaction. In particular, it provides in a straightforward manner analytic expressions for the scattering kernels,

$$\sigma(E_0, E) = \int_{4\pi} \frac{\partial^2 \sigma}{\partial \Omega \partial E} d\Omega \quad (4)$$

the total scattering cross section

$$\sigma(E_0) = \int_0^\infty \int_{4\pi} \frac{\partial^2 \sigma}{\partial \Omega \partial E} d\Omega dE \quad (5)$$

and the energy-transfer kernels [7-9]

$$\sigma_n(E_0, E) = \int_{4\pi} \frac{\partial^2 \sigma}{\partial \Omega \partial E} \cos^n(\theta) d\Omega \quad (6)$$

3. MODIFICATIONS TO THE NJOY CODE

In this section we briefly describe the modifications to NJOY in order to include the SSF formalism as an optional way to calculate cross sections for moderator materials.

The NJOY (94.105 version) code [10] received from RSIC was installed, as a test, on different platforms (PC, Sun Ultra with -r8 option, and Silicon Graphics). All the work presented here was done in a Sun-Ultra Spark 170 machine, with Solaris 2.5 operative system, and Fortran 77.

NJOY calculates the cross sections for moderators through two ways:

- Free-gas theory
- Calculation of the scattering matrix from the scattering law $S(\alpha, \beta)$ (calculated previously with LEAPR module) supplied in the ENDF/B-VI library.

The free-gas theory is not applicable to all the situations, while the scattering functions are available only for selected materials and temperatures, thus restricting the possibilities of nuclear data preparation to those cases.

The SSF formalism was written as a set of computer routines, which were tested through a range of application examples that involved the evaluation of neutron cross sections and thermalization properties of several moderator materials. Following the recommendations made at a recent meeting [11], we decided to tackle the problem of implementing the SSF into NJOY (94.105) as a third option to calculate cross sections for moderator materials.

Up to now, SSF input data sets are available for light and heavy water, liquid hydrogen (ortho and para), methane, glycerol, polyethylene, plexiglass, dodecane, TBP, benzene, dowtherm, metallic hydrides, but the data base will be extended in the future to other materials.

The main modifications were introduced in the THERMR module (subroutines CALCEM and SIGL, and function SIG), where new subroutines were added, adapting the formalism of the synthetic model to the NJOY system.

When NJOY calculates scattering kernels from the scattering function ($iinc = 4$) the initial energy grid is internally fixed (58 groups), and the final energy grid is calculated in an adaptively way, from the data provided in the $S(\alpha, \beta)$ tape. If the SSF is used ($iinc = 5$), the same grid of initial energies is adopted, and the same adaptive process is used for final energies determination, but from a fixed and extended grid of energy transfer (β). It consists of approximately 400 points, defined according to the values presented in ENDF/B-VI for the available moderators. The results obtained using that fixed extended grid for all the moderator materials, and using a specific one for each element were found to be in very good agreement.

Input modifications for the THERMR module:

→ In card 2, a new option for IINC was implemented. If IINC is equal to 5, the program will use the "Synthetic Scattering Module" (MODEL Subroutine) to compute the total cross section and the energy-transfer kernels.

→ In this case, new data are needed, which are given in card 5.

The first parameter (**I0**) indicates which material will be treated:

The meaning of the second and third parameters (**I1** and **I2**), depends on the material , because different routines might be used for different cases. For example, in the liquid hydrogen case, I1 can take the values 1, 2, or 3 if it is ortho-hydrogen, para-hydrogen or a mix of both materials, and I2 is read only in the case of I1.eq.3 giving the percentage of ortho-hydrogen in the mix. In any other case I1 indicates the type of cross section to be calculated, and I2 specify if the data will be for a molecule or for a single atom or atom family.

4. A FEW TYPICAL RESULTS

Applications of the SSF to a variety of hydrogeneous systems were presented in the past [12], where different magnitudes were predicted and compared with available experimental data or previous theoretical results.

In this work we present NJOY results for thermal neutron scattering kernels and total cross sections of water and methane, obtained from both its original ENDF/B-VI.2 library and the Synthetic Model formalism integrated in our modified version of the code.

4.1 Water at 300 K

We wanted to begin our comparison by looking at a classic –yet complex- system: room temperature water. As far as the SSF is concerned, its predictions for thermal cross sections and diffusion parameters have been comprehensively discussed and compared with existing information [4,6].

The Table 1 contains the input data for the Synthetic Model corresponding to hydrogen in water at 300 K. This set was adopted after a thorough analysis of measured frequency spectra with particular consideration of the internal modes' weights, especially for the low frequency part where the Sachs-Teller mass concept was used for normalization purposes [13]. Besides the two vibrational modes at 0.205 eV and 0.481 eV (that are almost the same as in the LEAPR input), the model uses a single Einstein oscillator at 0.07 eV to represent the actual broad rotational band, with a weight of 0.41667 (=7.5/18) rather than 0.44444 (=8/18).

Figure 1 shows the isotropic scattering kernels produced by NJOY using (a) its ENDF/B-VI.2 library and (b) the integrated SSF option. The great similarity between both sets is evident, besides some sharper features in the model-based result related to the crude approximation involved in representing the rotational band by a single oscillator. This fact is clearly displayed in Fig.2, where the ratio (b)/(a) is shown over the same group structure; the two thin 'walls' symmetric with respect to the diagonal correspond to creation and annihilation of that single rotational 'phonon'. Over the rest of the grid the ratio is essentially equal to one, except for some small departures (groups # 30-40) in regions where the value of the scattering kernel is not significant.

The scattering cross section of hydrogen in room temperature water is shown in Fig.3, where again a very good agreement is observed between the NJOY results based on ENDF/B-VI.2 and SSF over the full thermal energy range. There is however a small systematic discrepancy between both sets below 0.1 eV, that we cannot attribute to the Synthetic Model in view of its excellent agreement with experimental data on the total cross section of water [14]. Finally, we display in Fig.4 the behaviour of the two curves in the high-energy range, showing that the ENDF/B-VI.2 evaluation is a little low, as pointed out by MacFarlane [15]; on the other hand, the SSF curve naturally approaches the free-gas (at the proper 'effective temperature') result at eV energies.

4.2 Water at 1000 K

This system was considered to test the evolution of the two evaluations with the temperature, bearing in mind that water is one of the hydrogenous moderator with the largest temperature variation available in ENDF/B-VI.2. Concerning the SSF, it has been used in the past to predict diffusion parameters over a wide temperature range, showing good agreement with the existing integral measurements.

Another interesting point of discussion is related to the preparation of the input data for SSF. The set employed for water at 1000K is presented in Table 1, where only the two molecular vibrations enter as conforming the 'frequency spectrum', whereas the 'molecular mass' is the Sachs-Teller mass of hydrogen in the water molecule. The reason for that choice is that, in the spirit of the Synthetic Model, the single quantum oscillator representing the actual rotational band is highly excited at this temperature and therefore a quasi-classical treatment is applicable in this situation. In other words, whatever the energy of the incident neutron is, the latter will 'see' a scattering center which is part of a (thermally activated) freely-rotating molecule.

The NJOY calculated scattering kernels are shown in Fig.5, corresponding to (a) its ENDF/B-VI.2 evaluation and (b) the new SSF option. The two results are rather similar over the complete grid, except at the lower groups where the evaluation from the standard library is sharper, revealing an effective mass bigger than the Sachs-Teller mass used by the model. This fact is further emphasized in Fig.6, showing the ratio (b)/(a) which is very near to 1 everywhere but in the low energy region.

The cross section of hydrogen in this system is given in Fig.7, as produced by our NJOY version with its two options. Once again both curves are rather similar, although the SSF results are lower over most of the energy range. A more noticeable discrepancy is observed around 0.01 eV, presumably due to the lack of rotational quantum excitations in our model at this temperature (0.086 eV) which, after all, is not too high compared with the adopted characteristic energy (0.07 eV) for this motion (see Table 1) to ensure the attainment of the fully-rotating regime

As before, the approach to the free-gas limit is different for the two evaluations, as shown in Fig.8, where it seems again that ENDF/B-VI.2 produces a result too low at those high energies.

4.3 Methane at 100K

A great deal of work has been done on methane, prompted not only for being a theoretically accessible system [16], but also because of its interest as a cryogenic moderator for cold neutron sources [17]. Now, the SSF is particularly appropriate to describe a gas of spherical molecules, as CH₄ at room temperature. In this case, due to the very low energies associated to the molecular rotational motion, these modes are thermally excited and a quasi-classical treatment of them is applicable in the frame of the SSF formalism. Therefore, at all incident energies below the lower vibrational energy, the neutron will 'see' the hydrogen atoms as having a mass equal to their Sachs-Teller mass (3.4 amu); the effective temperature and vibrational factor over this region correspond to the system's temperature and the zero-point motion of the vibrational modes. Those three parameters (μ_0 , τ_0 , Γ) of the model (see Section 2) change as the neutron energy goes over the vibrations' energies (lumped into two Einstein oscillators at 0.17 eV and 0.38 eV) according to the model prescription [3].

The hypotheses discussed in the precedent paragraph are still valid for methane at 100K (~0.0086 eV), and in this sense the situation is equivalent to that of water at 1000K. The set of input data for the SSF is given in the Table 1.

In Fig.9 we present the results obtained for the scattering kernel of liquid methane (100 K) from the two options implemented in NJOY: (a) ENDF/B-VI.2 and (b) SSF. Some differences between both sets are apparent at the lower groups, reflecting the appropriate treatment of rotational and diffusive modes on which ENDF/B-VI.2 is based. However, as shown in Fig.10 for the ratio (b)/(a), those discrepancies are quite localized and with relatively small amplitudes.

The total scattering cross section of hydrogen in methane at 100 K is given in Fig.10 for the two evaluations. The agreement between them is not very good in this case, although the trend is similar. One may expect that at very low energies, the ENDF based calculation should give more reliable results, on account of its better description of the molecule's translation and rotations. In any case, it would be extremely useful to have experimental data over that range to elucidate this question.

In the intermediate region – at least from the point of view of the energy range covered by those NJOY calculations – the comparison between ENDF and SSF is shown in Fig.11, together with the experimental data of Rogalska [18]. The agreement between the measured points and the

Synthetic Model curve is excellent. Although this result can be confirmed at present only over a limited energy region, it is still important because that is about the expected peak position for the neutron flux emerging from a (large) liquid methane moderator, that will weigh most magnitudes of interest for neutronic calculations. Finally, the situation at high energies is shown in Fig.12, where the discrepancy observed in the previous cases is seen again here.

5. CONCLUSIONS

In this work we presented calculations performed using a modified version of the NJOY (94.105) code, in which a package of subroutines corresponding to the Synthetic Scattering Function formalism has been integrated as a new option. Results for a few moderators were used to illustrate the similarities and differences between the ENDF/B-VI.2 and SSF.

Although we have to benchmark the results based on this new option, besides the extensive applications already performed using the Synthetic Model, we expect that the powerful capabilities of this model to describe complex systems will become a useful tool after its integration into NJOY.

TABLE 1

Input data for the SSF. Energies are given in eV, and masses in amu.

	Mode 1	Mode 2	Mode 3	'Molec. Mass'
Water 300K				
Energy	0.07	0.205	0.481	18.011
Effect. mass	2.3999	4.8078	3.2066	
Water 1000K				
Energy	----	0.205	0.481	2.1177
Effect. mass	----	4.8078	3.2066	
Methane 100K				
Energy	----	0.170	0.380	3.4
Effect. mass	----	2.585	3.1344	

REFERENCES

- [1] S.W.Lovesey, *Theory of Neutron Scattering from Condensed Matter*, [Clarendon Press, Oxford, 1984].
- [2] A.C. Zemach and R.J. Glauber, Neutron Diffraction by Gases, *Phys.Rev.* **101**, 129 (1956).
- [3] J.R. Granada, Slow-neutron scattering by molecular gases: A Synthetic Scattering Function, *Phys.Rev.* **B31**, 4167 (1985).
- [4] J.R. Granada and V.H. Gillette, A Review of a Synthetic Scattering Function Approach to the Thermal and Cold Neutron Scattering Kernels of Moderator Materials *J.Neutron Research* , in press (1998).
- [5] J.R. Granada, V.H. Gillette and R.E. Mayer, Neutron cross sections and thermalization parameters for molecular gases using a synthetic scattering function, *Phys.Rev.* **A36**, 5585 (1987).
- [6] J.R. Granada, V.H. Gillette and R.E. Mayer, Neutron cross sections and thermalization parameters using a synthetic scattering function. II: Applications to H₂O, D₂O and C₆H₆, *Phys.Rev.* **A36**, 5594 (1987).
- [7] V.H. Gillette, PhD Thesis, Instituto Balseiro (Unpublished, 1989).
- [8] V.H. Gillette and J.R. Granada, Analytical scattering kernels of any order for molecular gases, *Proceedings of the VI CGEN*, (Rio de Janeiro, 1996).
- [9] M.K. Dede, A. Demény and J.K. Darai, Evaluation of neutron pulse measurements with Granada - Sibona plexiglass kernel, *Nucl.Instr.Meth.Phys.Res. A* **372**, 233 (1996).
- [10] R.E. MacFarlane and D.W. Muir, The NJOY Nuclear Data Processing System, Version 91, Los Alamos National Laboratory Report LA-12740-M (1994)
- [11] International Workshop on Cold Moderators for Pulsed Neutron Sources, Argonne National Laboratory (USA, 1997).
- [12] J.R. Granada and V.H. Gillette, Evaluation of thermal neutron cross section of moderator materials using a synthetic scattering function, *Physica B* **213&214**, 821 (1995).
- [13] D. Ravignani, Thermal Neutron Scattering from HDO, MSc Thesis (in Spanish), Instituto Balseiro, Univ.Nac.Cuyo (Unpublished, 1994).
- [14] J.R. Granada, R.E. Mayer and V.H. Gillette, Application of the Synthetic Scattering Function to the Design of Cold Moderators for Pulsed Neutron Sources: A Fast Response Methane Based Array, in Ref. [11].
- [15] R. MacFarlane, New Thermal Neutron Scattering Files for ENDF/B-VI Release 2, LANL Report LA-12639-MS.
- [16] A. K. Agrawal and S. Yip, Slow neutron scattering by molecular liquids, *Nucl.Sci.Eng.* **37**, 368 (1969).
- [17] Y. Kiyanagi *et al.*, Comparison of coupled liquid hydrogen and solid methane moderators for pulsed neutron sources, *Physica B* **213&214**, 857 (1995).
- [18] Z. Rogalska, Rotational dynamics of solid methane molecules by slow neutron cross section measurements, *Acta Phys.Polonica* **XXVII**, 581 (1965).

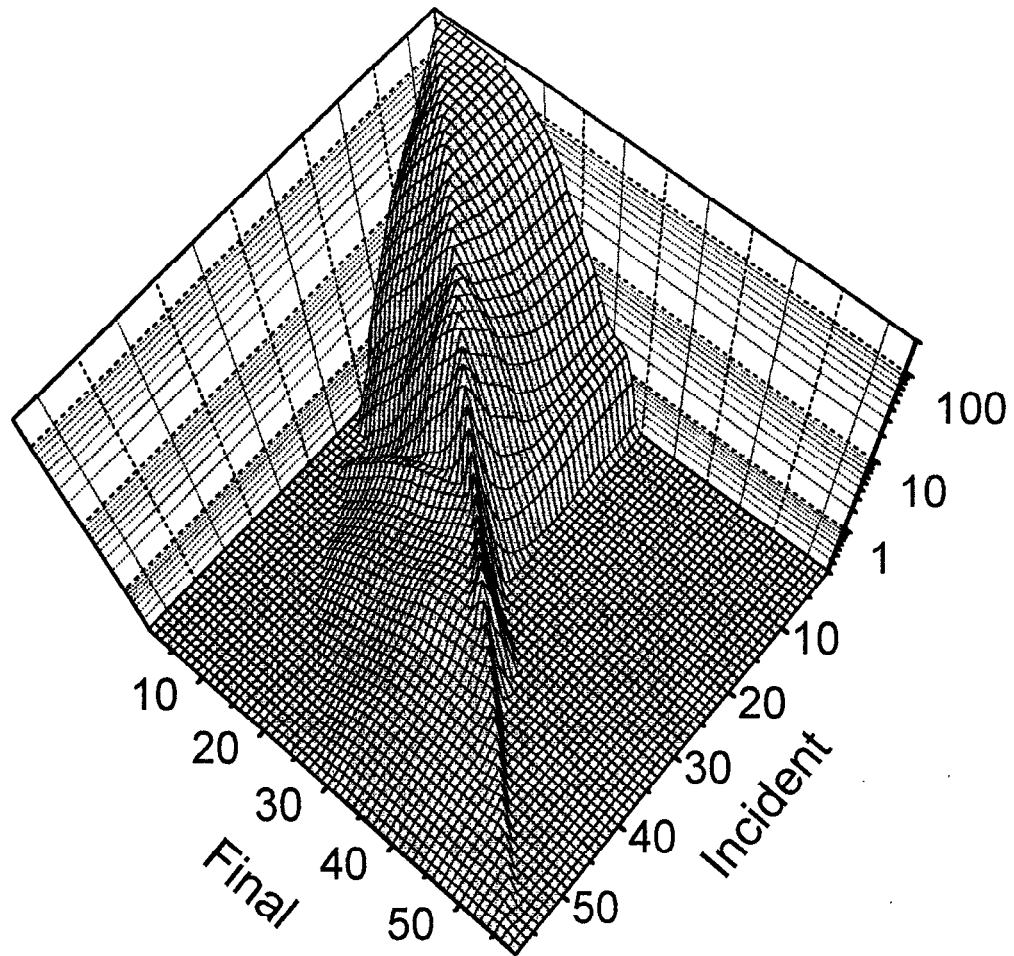


Fig.1(a): Scattering Kernel for H in H₂O at 300K, calculated by NJOY with option
(a) ENDF/B-VI.2

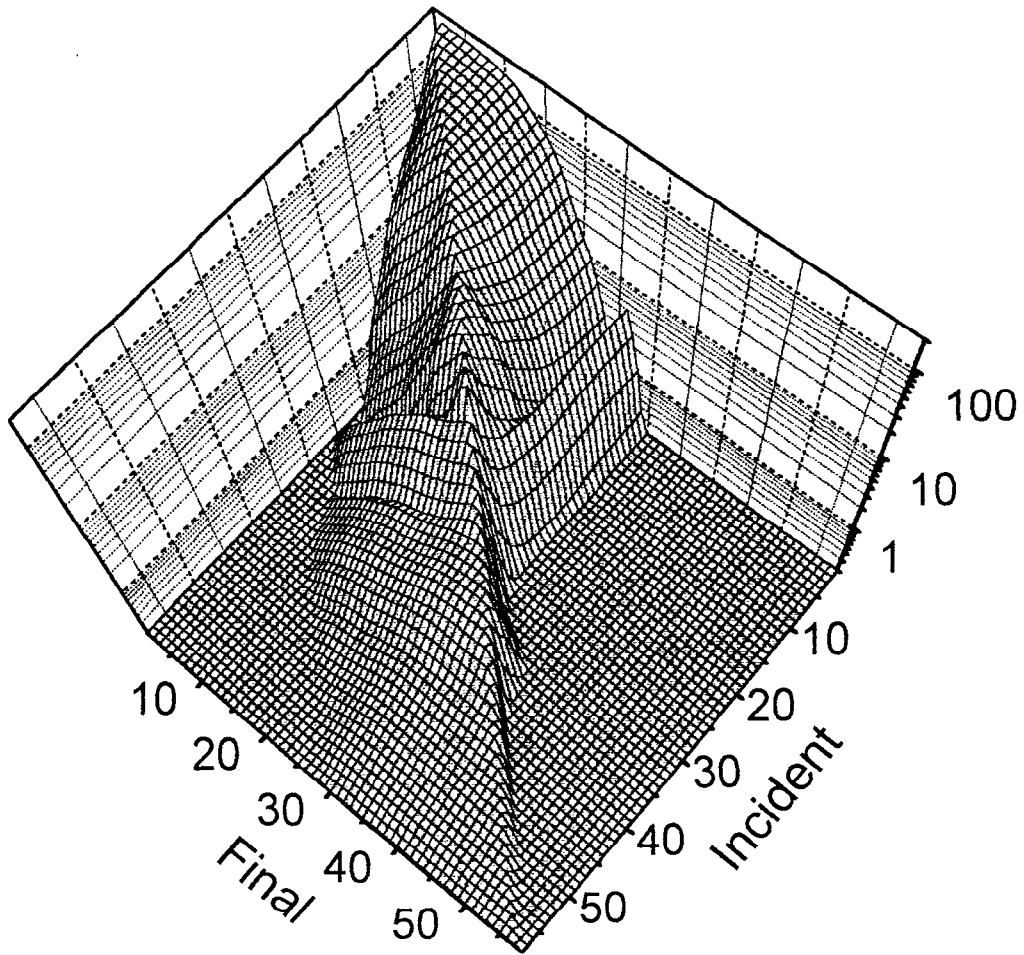


Fig.1(b): Scattering Kernel for H in H₂O at 300K, calculated by NJOY with option
(b) SSF

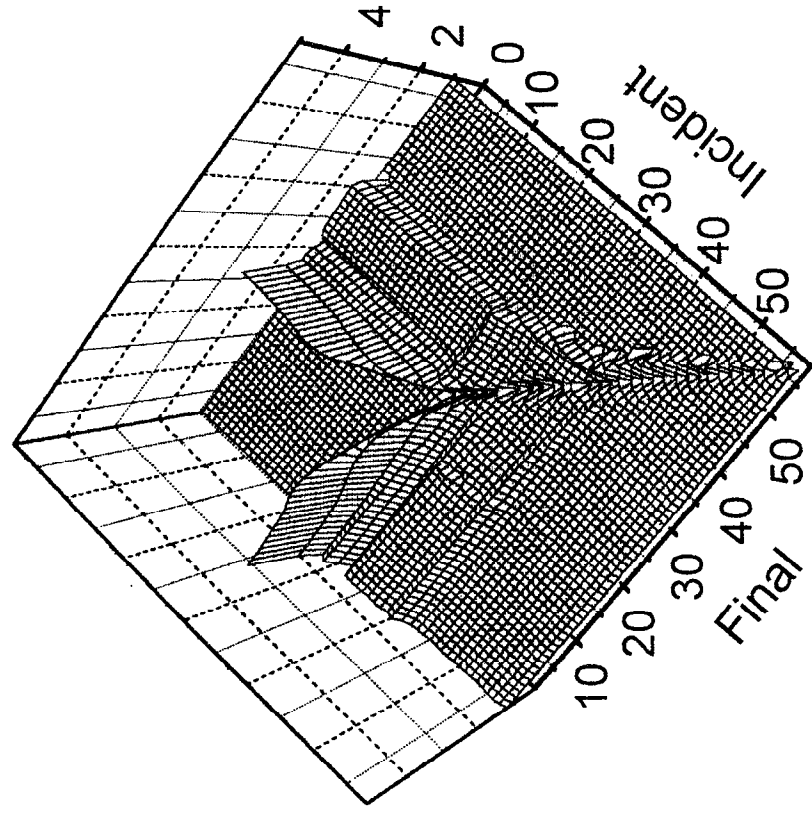


Fig.2: Ratio (b)/(a) of the Scattering Kernels for H in H₂O at 300K.

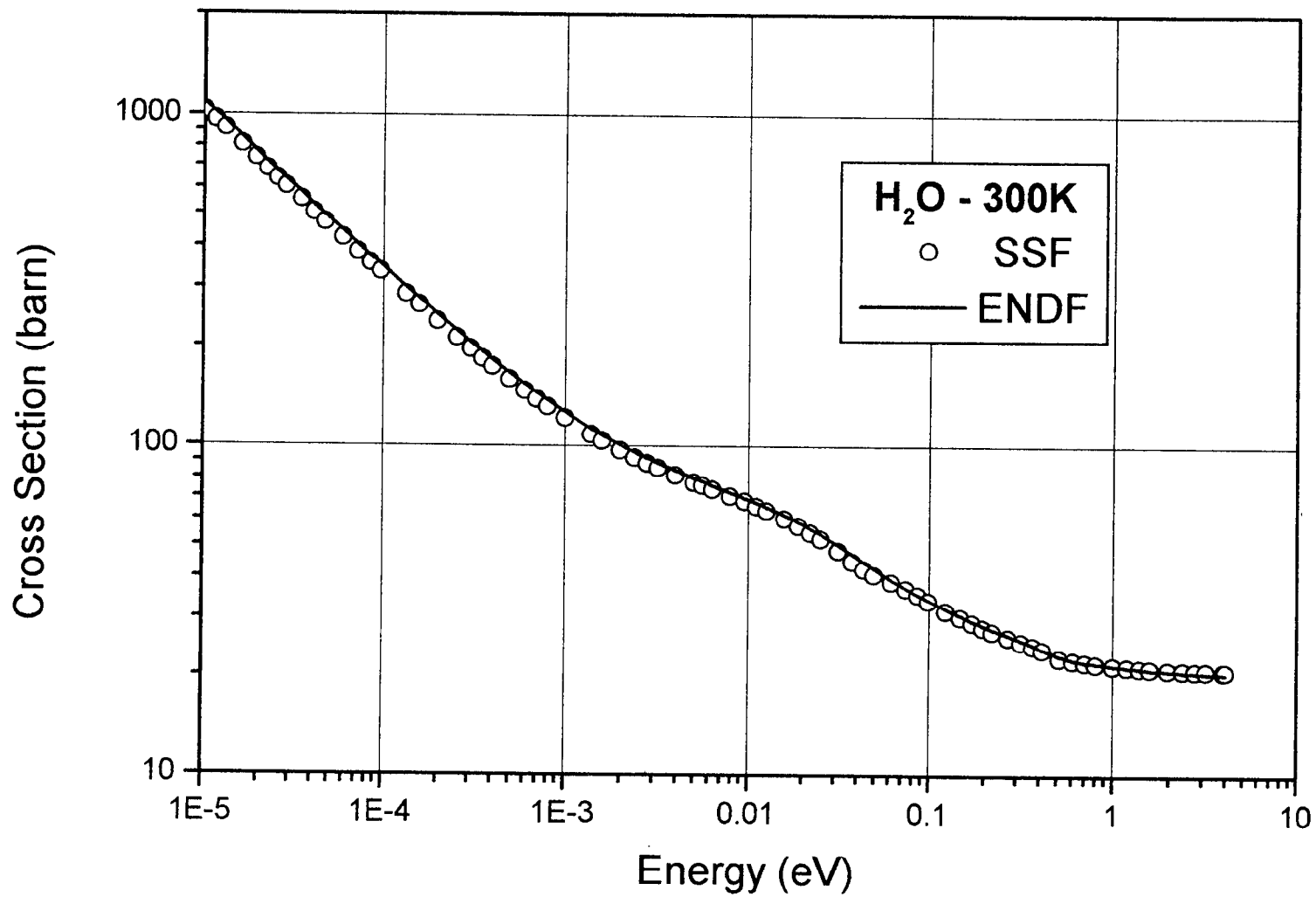


Fig.3: Cross section of H in H₂O at 300K calculated by our NJOY with its two options, over the full thermal energy range.

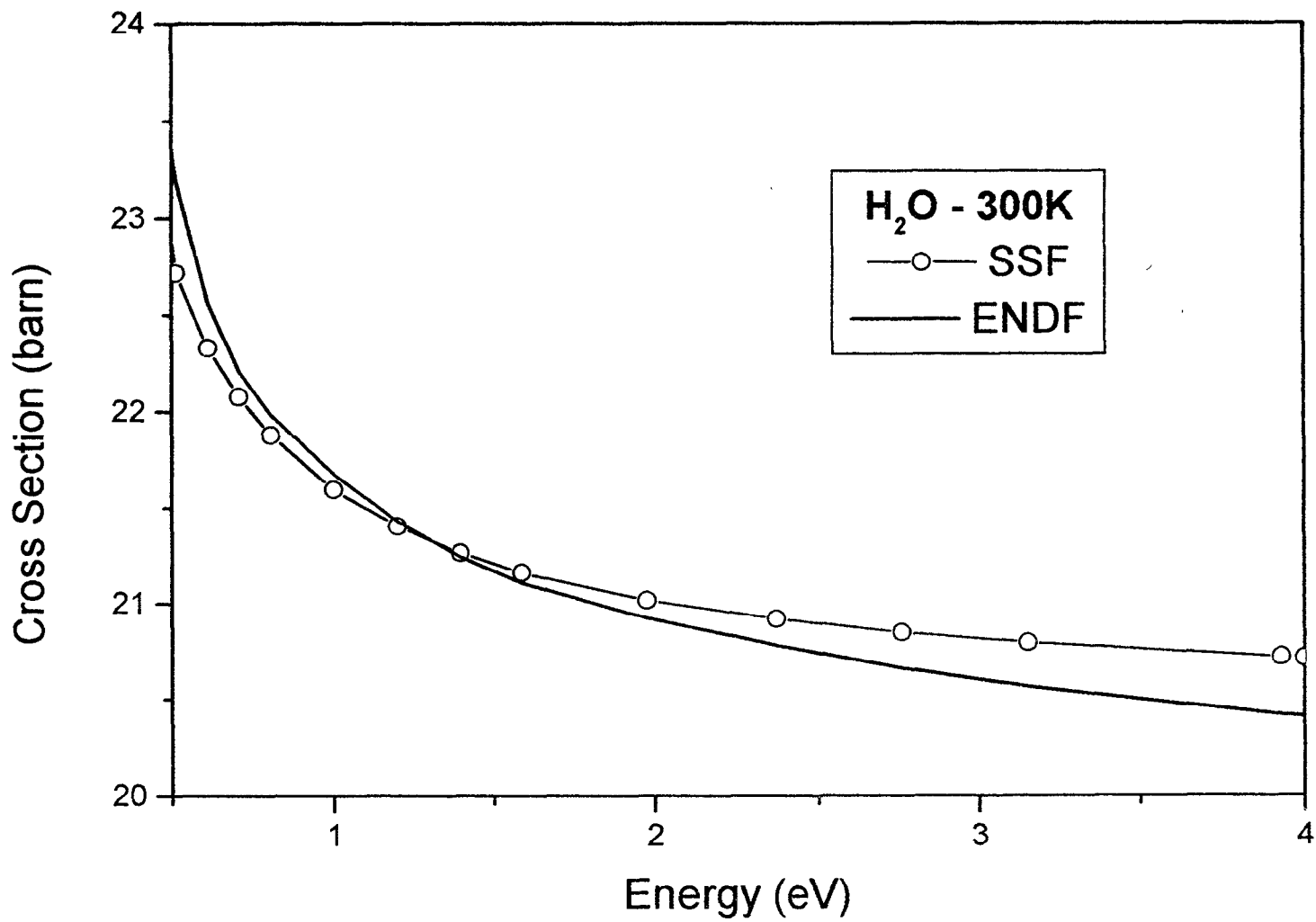


Fig.4: Cross section of H in H₂O at 300K calculated by our NJOY with its two options, over the high energy region.

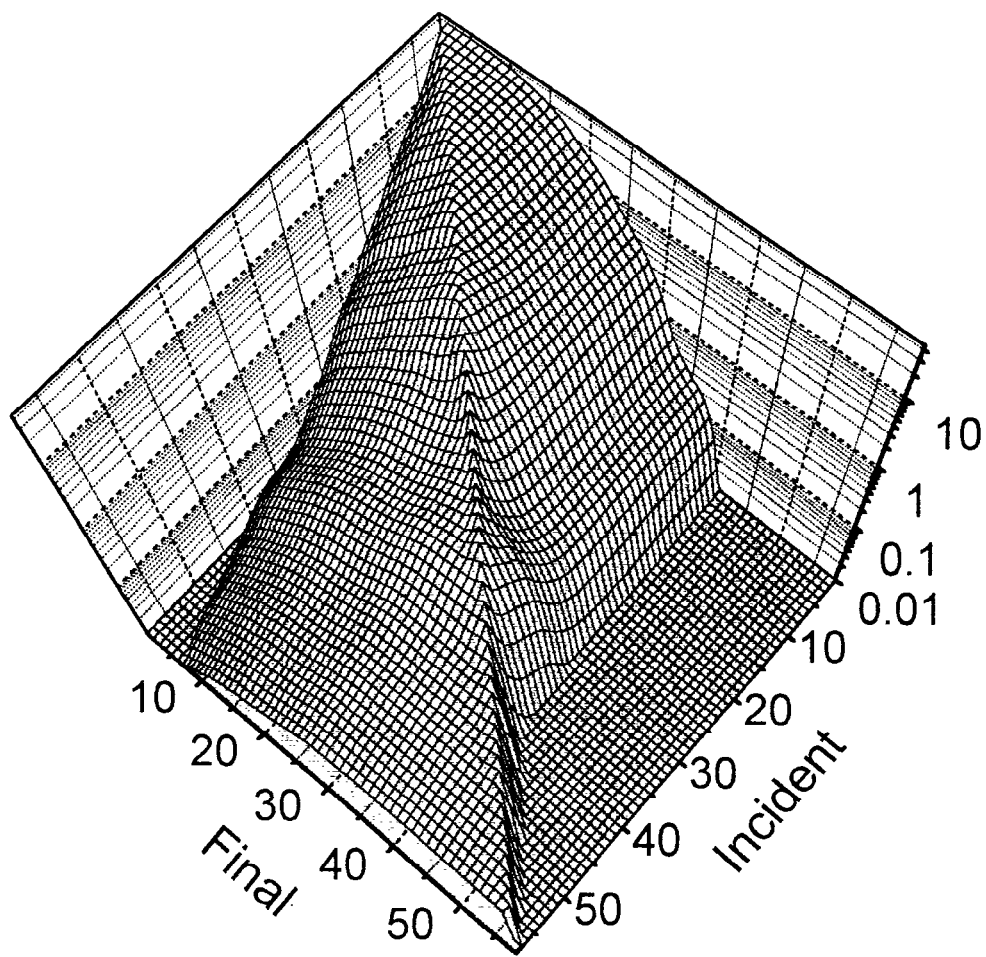


Fig.5(a): Scattering Kernel for H in H₂O at 1000K, calculated by NJOY with option
(a) ENDF/B-VI.2

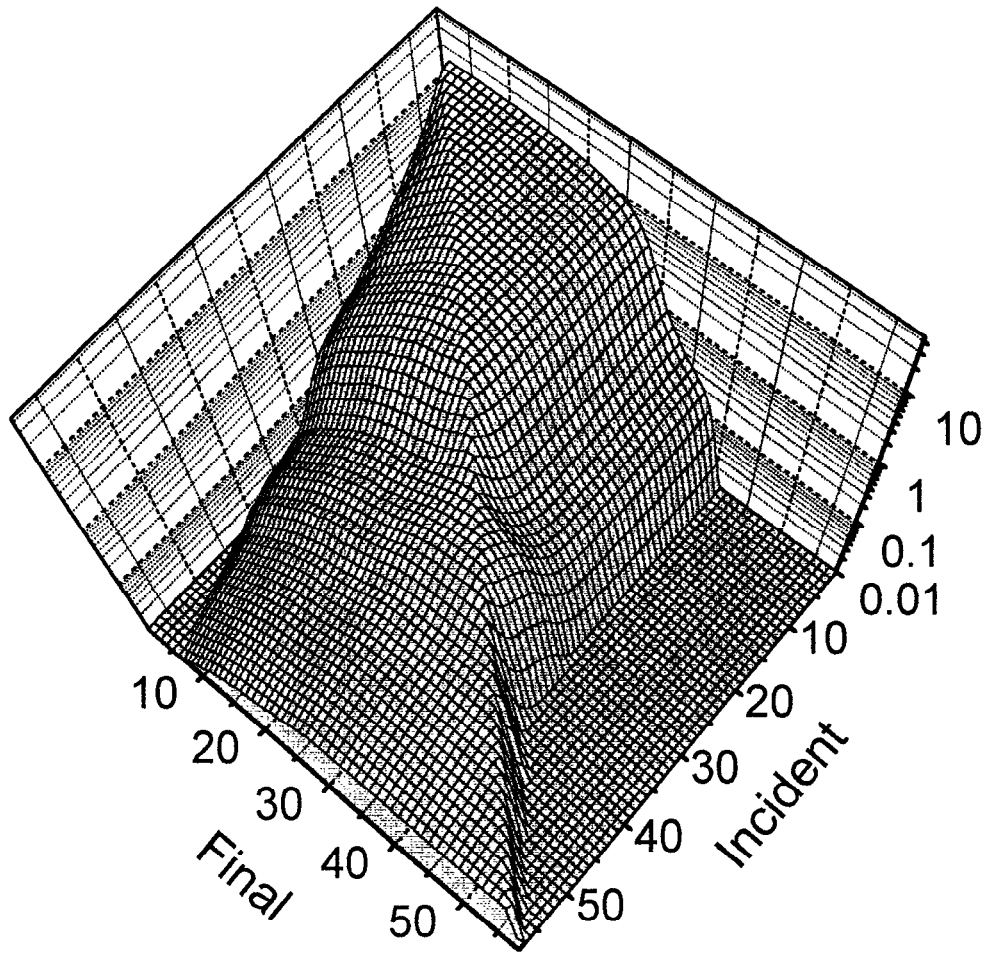


Fig.5(b): Scattering Kernel for H in H₂O at 1000K, calculated by NJOY with option (b) SSF

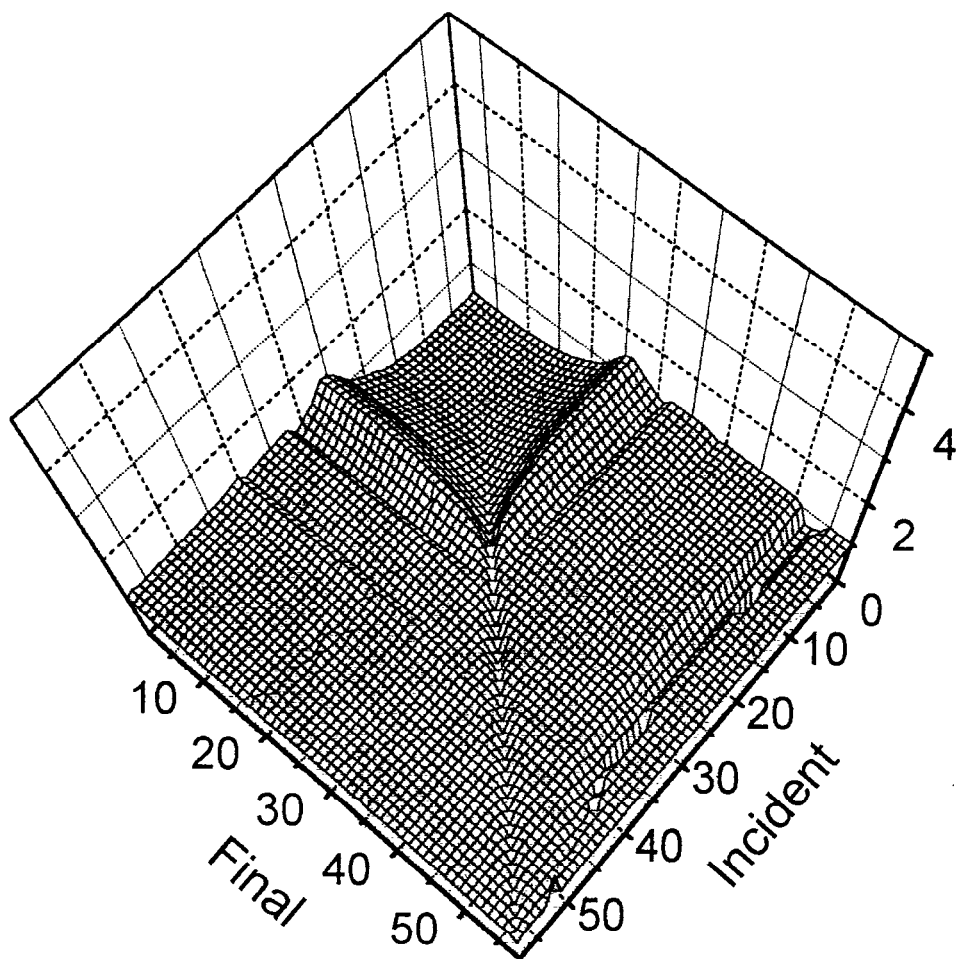


Fig.6: Ratio (b)/(a) of the Scattering Kernels for H in H₂O at 1000K.

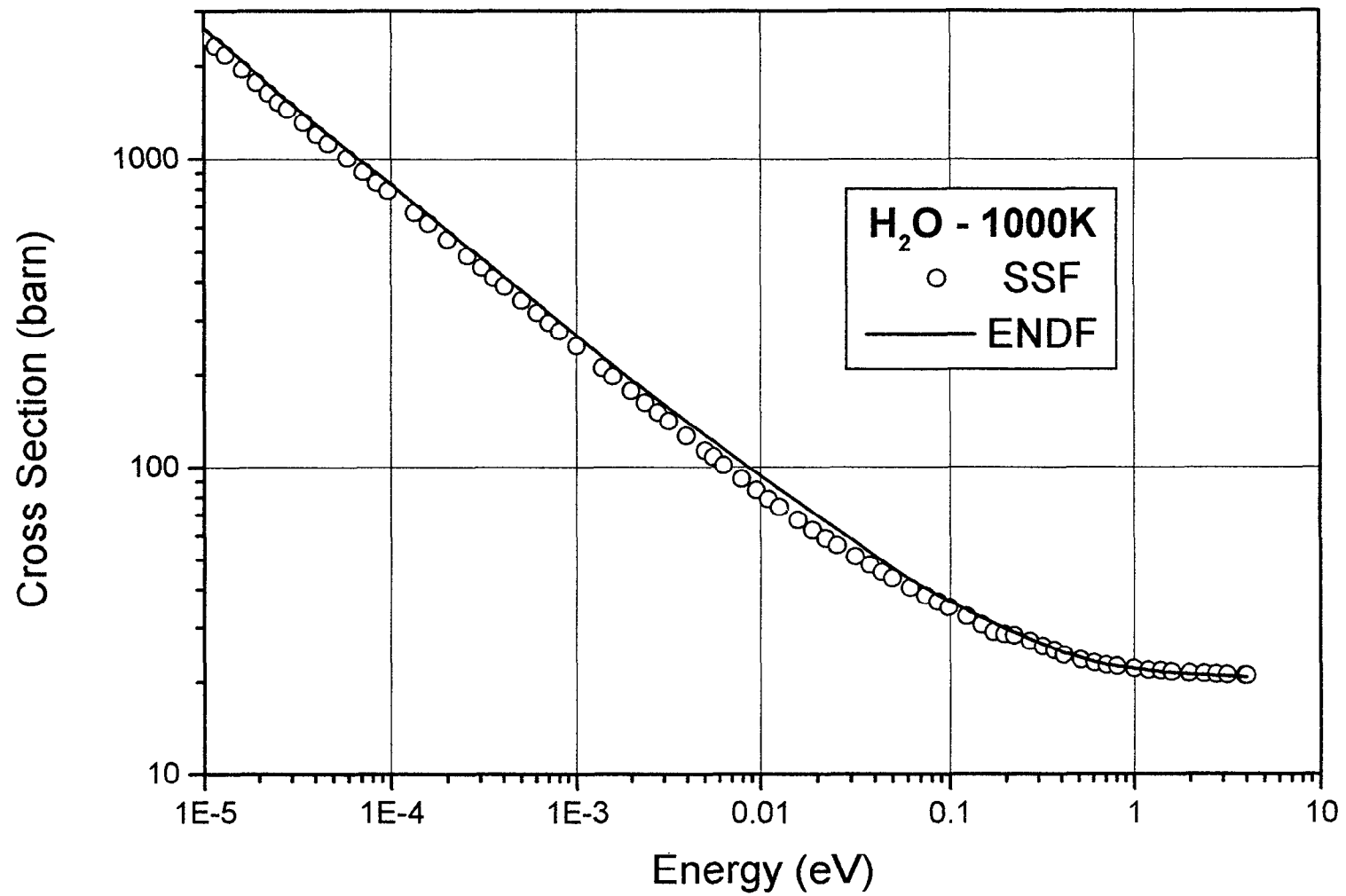


Fig.7: Cross section of H in H₂O at 1000K calculated by our NJOY with its two options, over the full thermal energy range.

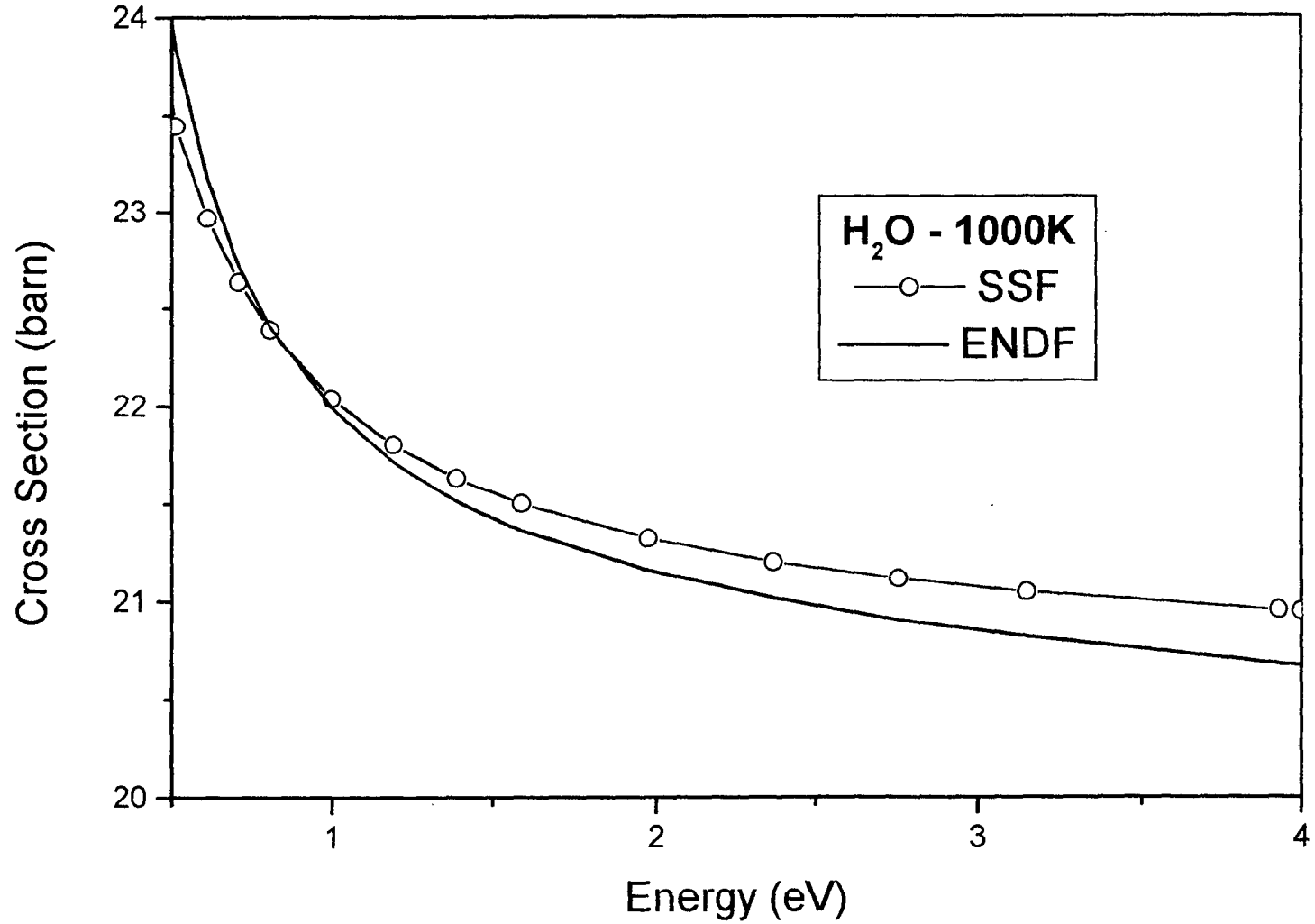


Fig.8: Cross section of H in H₂O at 1000K calculated by our NJOY with its two options, over the high energy region.

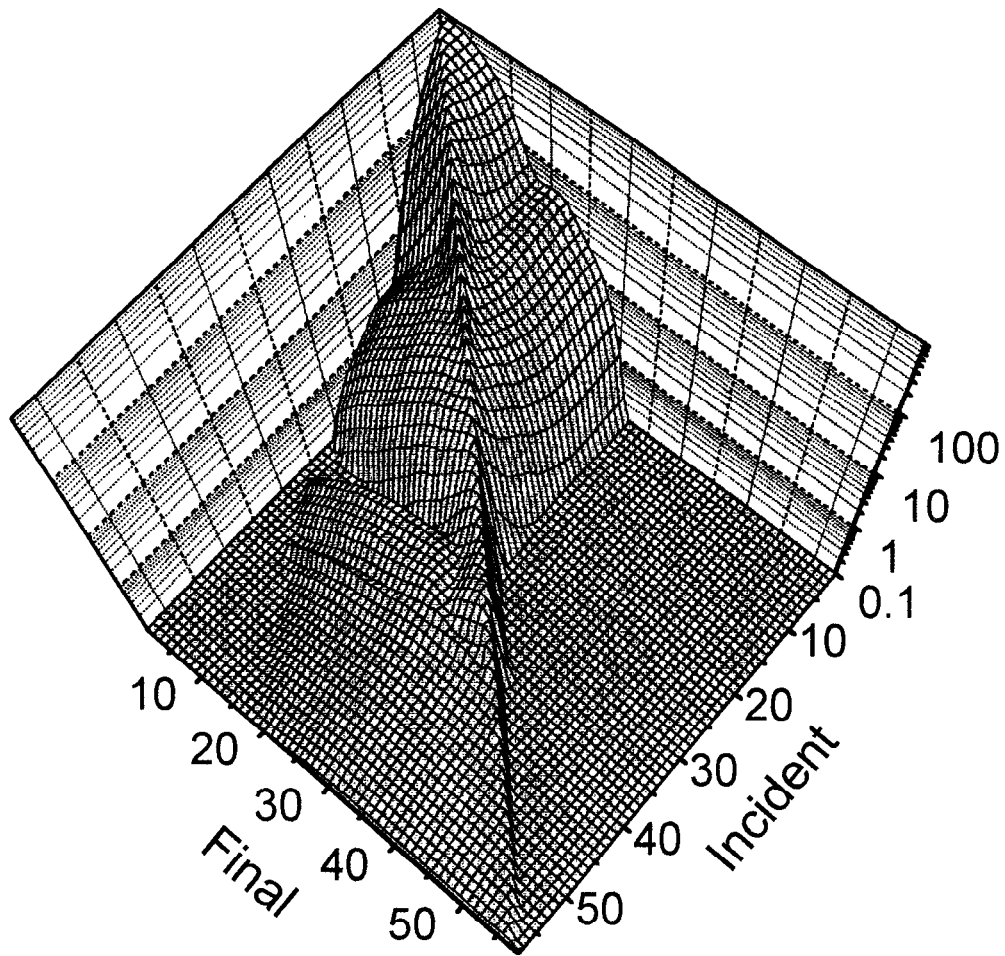


Fig.9(a): Scattering Kernel for H in CH₄ at 100K, calculated by NJOY with option
(a) ENDF/B-VI.2

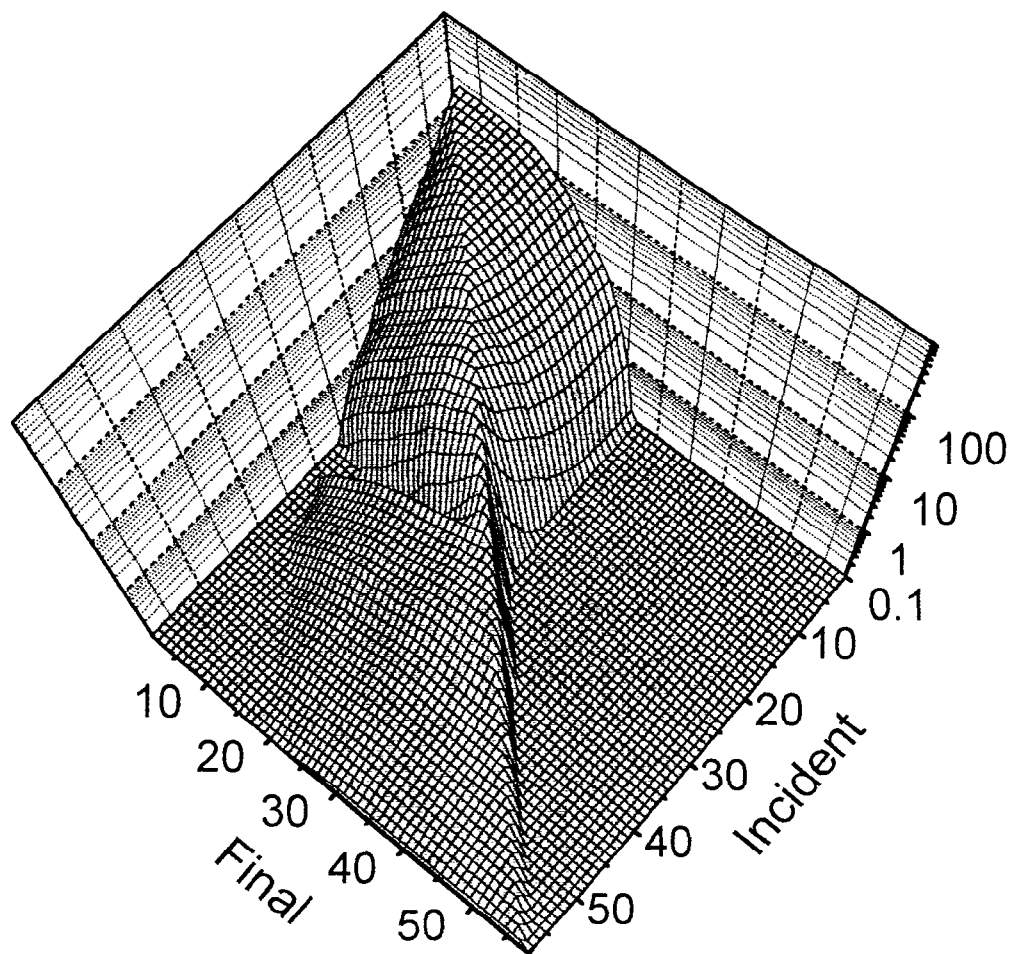


Fig.9(b): Scattering Kernel for H in CH₄ at 100K, calculated by NJOY with option (b) SSF

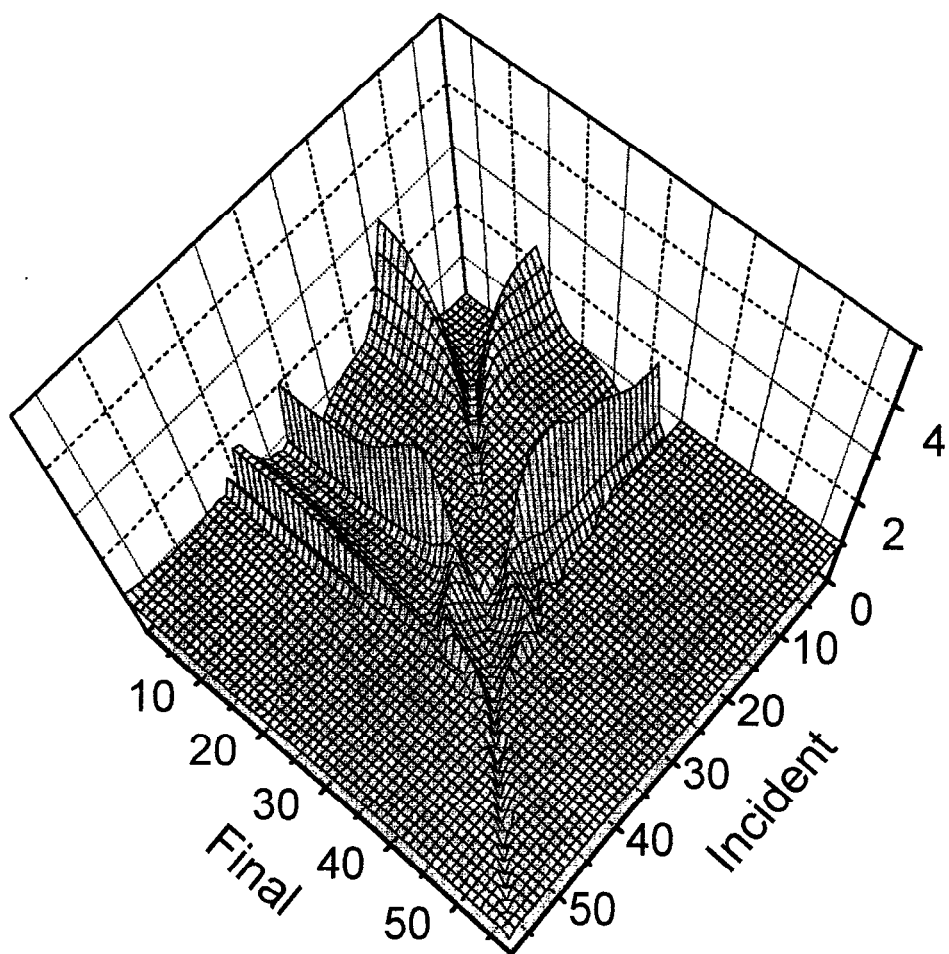


Fig.10: Ratio (b)/(a) of the Scattering Kernels for H in CH₄ at 100K.

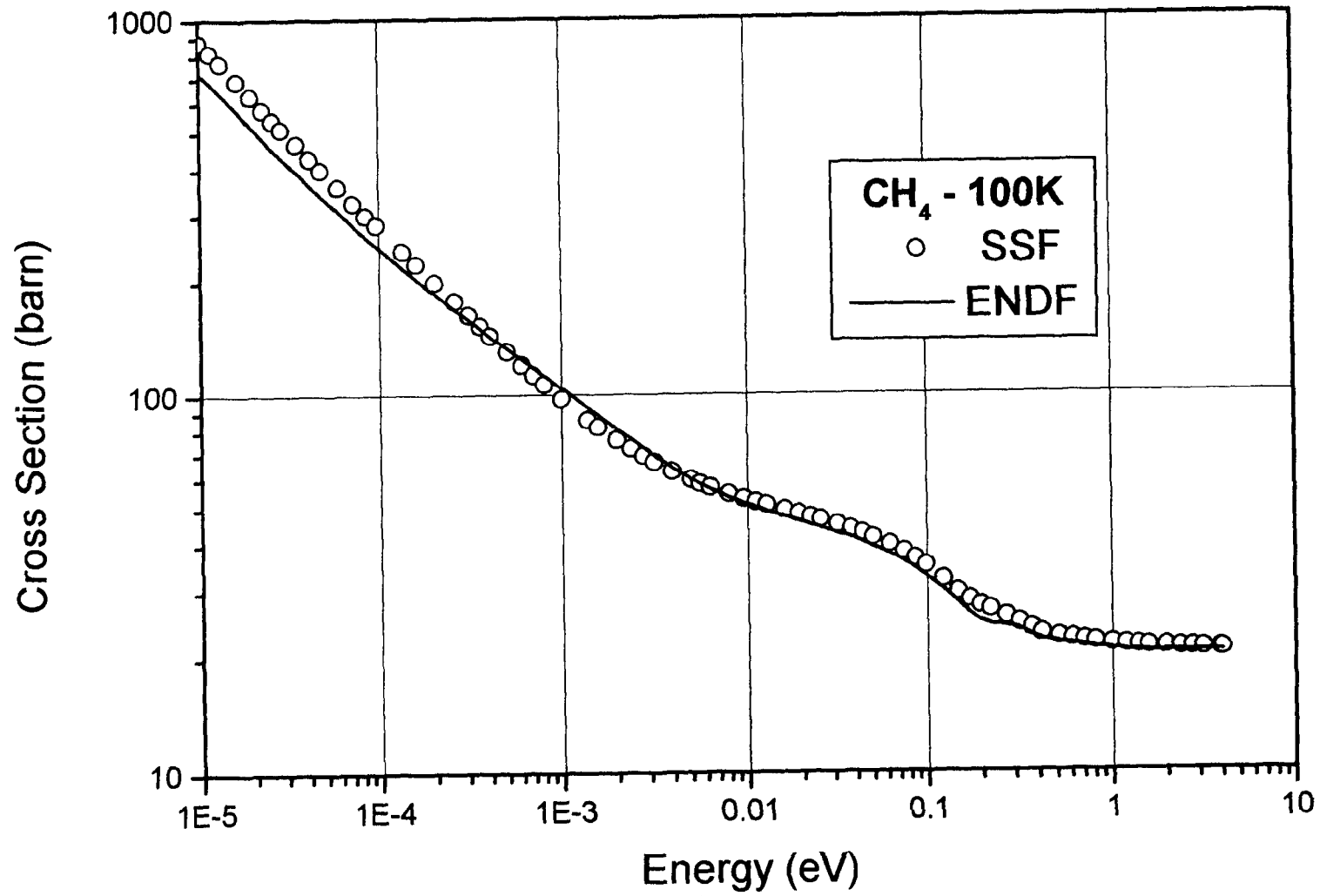


Fig.11: Cross section of H in CH₄ at 100K calculated by our NJOY with its two options, over the full thermal energy range.

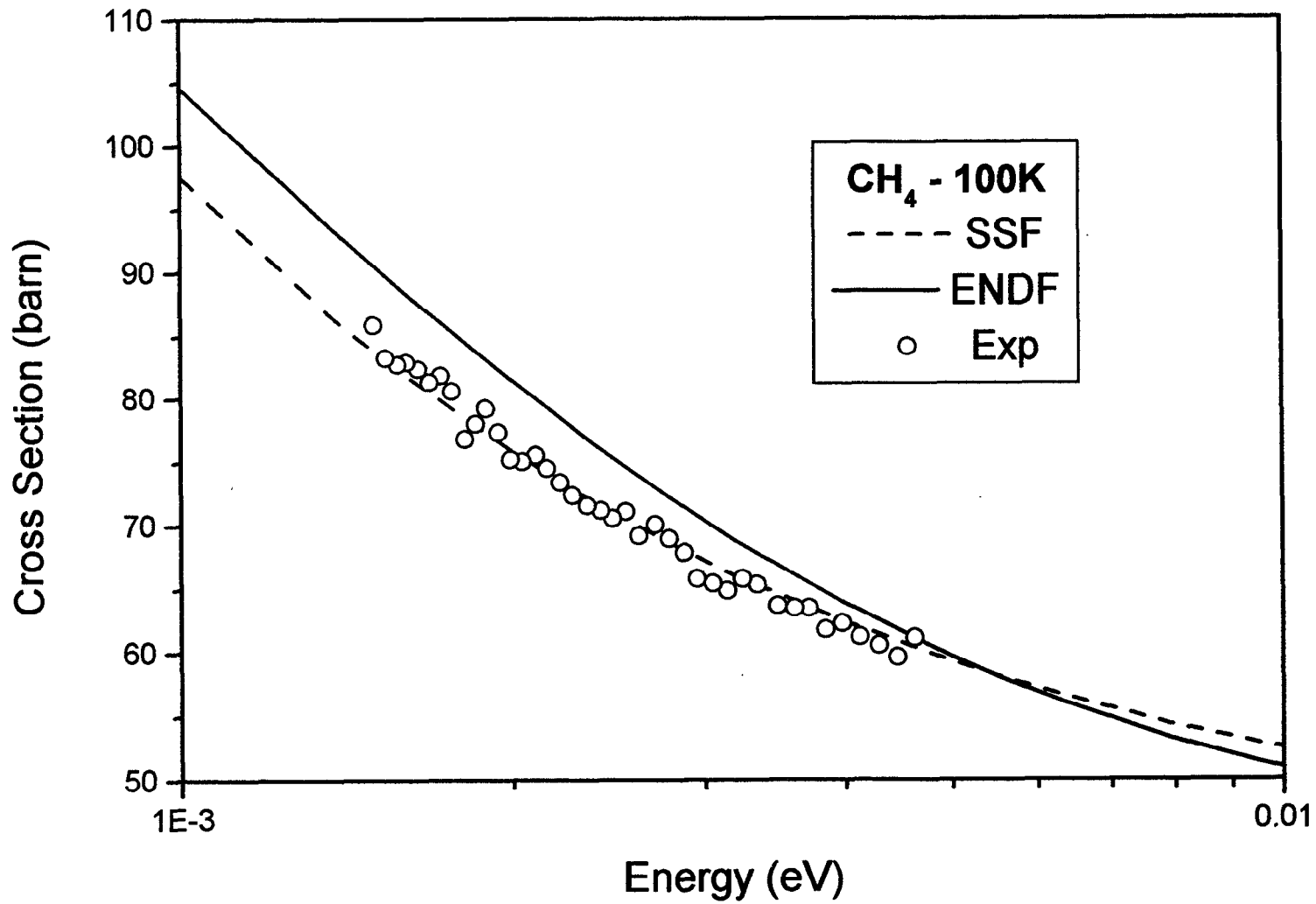


Fig.12: Cross section of H in CH₄ at 100K calculated by our NJOY with its two options, over the intermediate energy range.

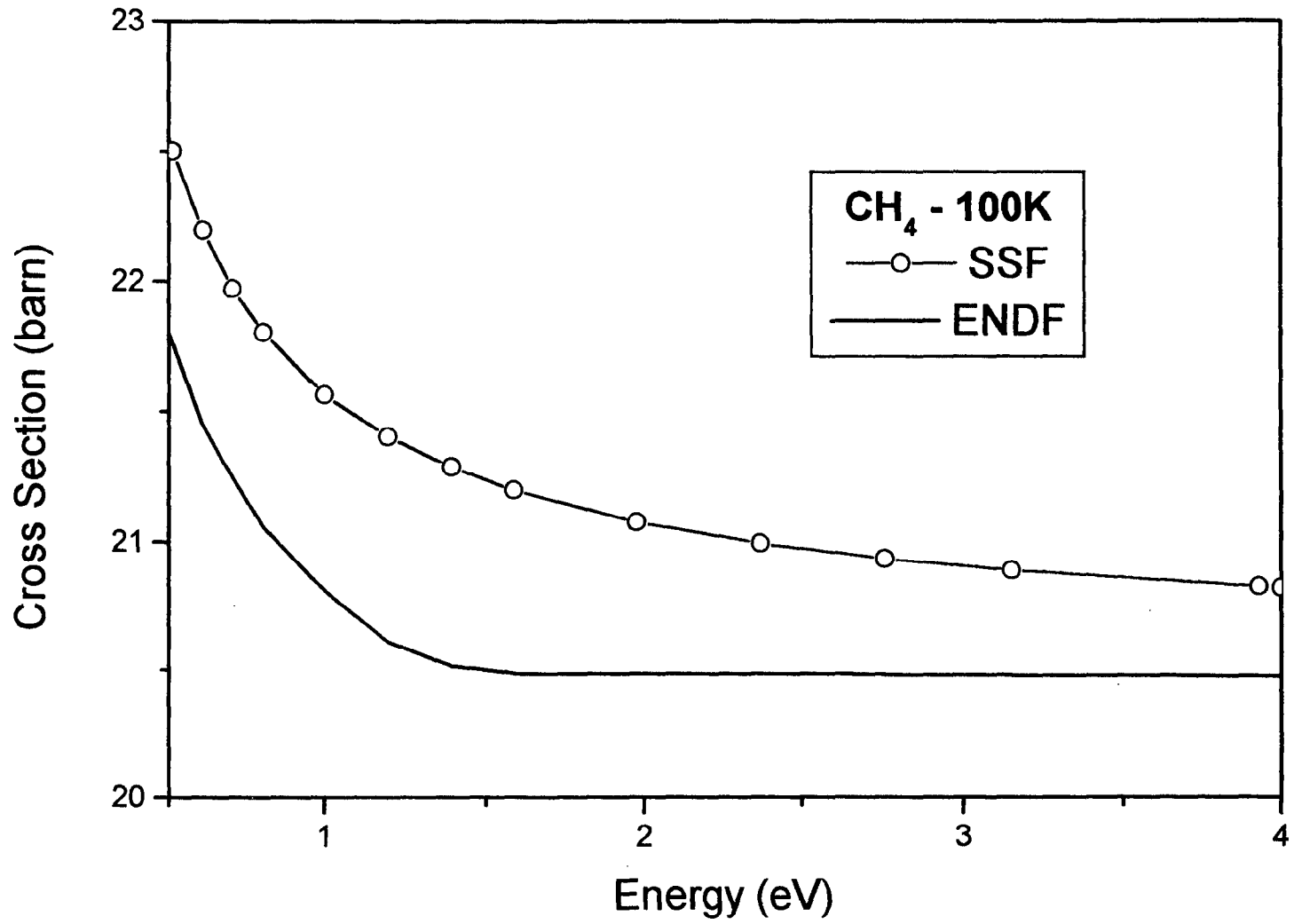


Fig.13: Cross section of H in CH₄ at 100K calculated by our NJOY with its two options, over the high energy region.